ELSEVIER

Chemical Engineering Journal 112 (2005) 181–190

Chemical Engineering Journal

www.elsevier.com/locate/cej

The biosorption of Acid Red 337 and Acid Blue 324 on *Enteromorpha prolifera*: The application of nonlinear regression analysis to dye biosorption

Ayla Özer[a,*], Gönül Akkaya[a], Meral Turabik[b]

[a] *University of Mersin, Department of Chemical Engineering, 33343 Çiftlikköy-Mersin, Turkey*
[b] *University of Mersin, Higher Vocational School of Mersin, 33343 Çiftlikköy-Mersin, Turkey*

Received 21 March 2005; received in revised form 1 July 2005; accepted 12 July 2005

Abstract

The biosorption of Acid Red 337 and Acid Blue 324 from aqueous solution on *Enteromorpha prolifera* was investigated in a batch system. Optimum initial pH and temperature values for AB 324 and AR 337 dyes were found as 3.0 and 2.0, 25 and 30 °C, respectively and the optimum dye uptake amounts per unit mass were obtained at 0.5 g/l biosorbent concentration for both dyes. The Langmuir, Freundlich and Redlich–Peterson adsorption models were applied to experimental equilibrium data and the isotherm constants were calculated using Polymath 4.1 software. The monolayer covarage capacities of *E. prolifera* for AB 324 and AR 337 were obtained as 160.6 and 210.9 mg/g, respectively. It was observed that the biosorption data fitted well to Redlich–Peterson model than the other models. The external diffusion and intraparticle diffusion models were also applied to biosorption data of AR 337 and AB 324 and it was found that both the surface adsorption as well as intraparticle diffusion contribute to the actual adsorption process. The constants obtained from the pseudo-second order kinetic model at different temperatures were evaluated and the activation energies for the biosorption of AB 324 and AR 337 were found to be −31.5 and −19.87 kJ/mol, respectively. Thermodynamic parameters such as enthalpy, entropy and Gibb's free energy changes were also calculated and it was concluded that the biosorption of these acidic dyes on *E. prolifera* was exothermic in nature.

Keywords: Biosorption; Isotherm; Nonlinear regression; Pseudo-second order kinetics; Weber–Morris model

1. Introduction

Dyes are synthetic aromatic water-soluble dispersible organic colorants, having potential application in various industries [1]. Textile industry (and especially its part focused on the dyeing process) belongs among important sources of contamination responsible for the continuous pollution of the environment [2]. The effluents of these industries are highly coloured and disposal of these wastes into the environment can be extremely deleterious [3]. Wastewaters containing dye may be toxic and even carcinogenic and this posses a serious hazard to aquatic living organisms [1,3]. The presence of dyes in water reduces light penetration and has a derogatory effect on photosynthesis. There are more than 100,000 dyes available commercially, most of which are difficult to decolorize due to their complex structure and synthetic origin [4,5]. They are specifically designed to resist fading upon exposure to sweat, light, water and oxidizing agents, and as such very stable and difficult to degrade [6]. Of current world production of dyestuffs of 10 million kg/year between 1 and 2 million kg of active dye enter the biosphere, either dissolved or suspended in water, every year [7]. It is evident, therefore, that removal of such coloured agents from aqueous effluents is of significant environmental, technical and commercial importance [8].

The conventional methods for treating dye-containing wastewaters are coagulation and flocculation, reverse osmosis, electroflotation, membrane filtration, irradiation and

* Corresponding author.
E-mail address: ayozer@mersin.edu.tr (A. Özer).

1385-8947/$ – see front matter © 2005 Elsevier B.V. All rights reserved.
doi:10.1016/j.cej.2005.07.007

Nomenclature

a_{RP}	Redlich–Peterson isotherm constant (l/mg)
C	dye concentration at any time t (mg/l)
C_{ad}	adsorbed dye concentration (mg/l)
C_{eq}	unadsorbed dye concentration in solution at equilibrium (mg/l)
C_0	initial dye concentration (mg/l)
E_A	activation energy of adsorption (kJ/mol)
ΔG	free energy change (kJ/mol)
ΔH	enthalpy change (kJ/mol)
k_0	temperature independent factor (g/mg min)
$k_{2,ad}$	pseudo-second order rate constant of sorption (g/mg min)
K	intraparticle rate constant (mg/g min$^{1/2}$)
K_a	constant related to the affinity of the binding sites (l/mg)
K_F	adsorption capacity
K_L	Langmuir constant (obtained by multiplying Q^0 and K_a) (l/mg)
K_{RP}	Redlich–Peterson isotherm constant (l/g)
n	adsorption intensity
q_{eq}	amount of adsorbed dye per unit weight of biomass at equilibrium (mg/g)
q_t	amount of adsorbed dye on the surface of the adsorbent at any time t (mg/g)
Q^0	maximum amount of the dye per unit weight of biomass to form a complete monolayer on the surface bound at high C_{eq} (mg/g)
R	universal gas constant, 8.314 (J/mol K)
R^2	correlation coefficient
S	specific surface area for the mass transfer (cm^2/g)
ΔS	entropy change (kJ/mol K)
T	absolute temperature (K)
X_0	biosorbent concentration (g/l)

Greek letters

β	exponent in Redlich–Peterson isotherm
β_I	external film diffusion coefficient (cm/min)

ozonation and active carbon adsorption [9]. The most popular of these technologies is activated carbon adsorption and widely used but it is expensive. Therefore, there is a growing interest in using low-cost, easily available materials for the adsorption of dye colours [10].

The term 'biosorption' refers to different modes involving a combination of active and passive transport mechanism to remove unwanted materials by microbial biomass. The use of inactivated biomass is advantageous as the process is free from nutrient supply and moreover there are no toxicity constraints in the organism employed [10,11]. Recent investigations by various groups have shown that selected species of seaweeds possess impressive adsorption capacities for a range of heavy metal ions but there is few studies on the colour removal [11]. Seaweeds are a widely available source of biomass as over 2 million tonnes are either harvested from oceans or cultured annually for food or phycocolloid production [12]. In this study, the biosorption of Acid Red 337 and Acid Blue 324 dyes, known as the components of textile industry wastewaters, on *Enteromorpha prolifera*, growing on Mediterranean cost in Mersin, Turkey, was studied in a batch system and experimental data were evaluated using nonlinear regression programme of Polymath 4.1 software which uses Levenberg–Marquardt algorithm for finding the parameter values which minimize the sum of the squares of the errors (ERRSQ).

2. Theory

2.1. Equilibrium of biosorption

The successful representation of the dynamic adsorptive separation of solute from solution onto an adsorbent depends upon a good description of the equilibrium separation between the two phases. Adsorption equilibrium is established when the amount of solute being adsorbed onto the adsorbent is equal to the amount being desorbed [7]. It is possible to depict the equilibrium adsorption isotherms by plotting solid phase concentration (q_{eq}; mg/g) against liquid phase concentration (C_{eq}; mg/l) of solute. Several isotherm models were used to describe the equilibrium between adsorbed dye molecules on the algal cell and dye molecules in solution at constant temperature.

2.1.1. Langmuir isotherm

The Langmuir model is valid for monolayer adsorption onto a surface with a finite number of identical sites. The well-known expression of the Langmuir model is given by Eq. (1):

$$q_{eq} = Q^0 K_a C_{eq}/(1 + K_a C_{eq}) \quad (1)$$

where q_{eq} (mg/g) and C_{eq} (mg/l) are the amount of adsorbed dye per unit weight of biomass and unadsorbed dye concentration in solution at equilibrium, respectively. Q^0 is the maximum amount of the dye per unit weight of biomass to form a complete monolayer on the surface bound at high C_{eq} (mg/l) and K_a is the adsorption equilibrium constant (l/mg). Q^0 represents a practical limiting adsorption capacity when the surface is fully covered with dye molecules and it assists in the comparison of adsorption performance, particularly in cases where the sorbent did not reach its full saturation in experiments.

2.1.2. Freundlich isotherm

The Freundlich expression (Eq. (2)) is an exponential equation and therefore, assumes that as the adsorbate concentration increases, the concentration of adsorbate on the

adsorbent surface also increases [7]. Theoretically using this expression, an infinite amount of adsorption can occur:

$$q_{eq} = K_F C_{eq}^{1/n} \quad (2)$$

In this equation, K_F and $1/n$ are the Freundlich constants characteristic on the system, indicating adsorption capacity and intensity, respectively.

2.1.3. Redlich–Peterson isotherm

The three parameter Redlich–Peterson equation has been proposed to improve the fit by the Langmuir or Freundlich equation and is given by Eq. (3).

$$q_{eq} = K_{RP} C_{eq} / (1 + a_{RP} C_{eq}^{\beta}) \quad (3)$$

where K_{RP}, a_{RP} and β are the Redlich–Peterson parameters. β lies between 0 and 1. For $\beta = 1$, Eq. (3) converts to the Langmuir form [7,13]. The three parameters Redlich–Peterson isotherm was evaluated using nonlinear least squares method.

2.2. Pseudo-second order kinetic model

The sorption kinetics describe the solute uptake rate which, in turn, controls the residence time of sorbate uptake at the solid–solution interface. Therefore, it is important to be able to predict the rate at which the pollutant is removed from aqueous solutions in order to design appropriate sorption treatment plants [14]. According to literature, pseudo-second order kinetics is more available for the dyestuff biosorption than the other kinetic models since the effects of transport phenomena and chemical reactions are often experimentally inseperable [8,9,11]. The main assumption of the pseudo-second order kinetic model is that the sorption capacity is proportional to the number of active sites occupied on the sorbent, then the kinetic rate law can be written as follows:

$$dq_t/dt = k_{2,ad}(q_{eq} - q_t)^2 \quad (4)$$

where $k_{2,ad}$ is the rate constant of sorption (g/mg min), q_{eq} the amount of adsorbed species at equilibrium (mg/g) and q_t is the amount of adsorbed species on the surface of the sorbent at any time t (mg/g). Separating the variables in Eq. (4) gives:

$$dq_t/(q_{eq} - q_t)^2 = k_{2,ad}\, dt \quad (5)$$

Integrating this for the boundary conditions $t = 0$–t and $q_t = 0$–q_t gives:

$$1/(q_{eq} - q_t) = 1/q_{eq} + k_{2,ad} t \quad (6)$$

Eq. (6) can be rearranged to obtain:

$$t/q_t = (1/k_{2,ad} q_{eq}^2) + (t/q_{eq}) \quad (7)$$

where q_{eq} and $k_{2,ad}$ values can be determined by using Polymath 4.1 software.

2.3. Mass transfer models

If the movement of dye from the bulk liquid to the liquid film surrounding the adsorbent is ignored, the adsorption process in porous solids can be separated into three stages: The first stage is diffusion through the solution to the external surface of the adsorbent and also called film mass transfer or boundary layer diffusion of solute molecules. The second stage is diffusion within the pores or capillaries of the adsorbent internal structure to the sorption sites where the third stage of rapid uptake occurs [15–17]. The last step is assumed to be rapid while steps 1 and 2 are the rate determining steps, either singly or in combination [13].

2.3.1. Weber–Morris model

In a diffusion controlled adsorption process, the adsorbed amount of the solute varies almost proportionately with a function of retention time, $t^{1/2}$ as early mentioned by Weber and Morris:

$$q_t = K t^{1/2} \quad (8)$$

According to this model, the plot of uptake (q_t) versus the square root of time should be linear if intraparticular diffusion is involved in the adsorption process and if these lines pass through the origin then intraparticle diffusion is the rate controlling step [15,16]. In many cases, an initial steep-sloped portion indicating external mass transfer is followed by a linear portion to the intraparticle diffusion and plateu which represents the final equilibrium stage where the intraparticular diffusion starts to slow down due to exteremely low solute concentration in the solution and surface [15,17,18].

2.3.2. Frusawa and Smith model

The external mass transfer coefficients for the dye biosorption were determined using a diffusion model referred as the F&S (Frusawa and Smith) model [19,20]:

$$C_t/C_0 = 1/(1 + mK_L) + (mK_L/1 + mK_L) \times \exp[(-(1 + mK_L)/mK_L)\beta_I St] \quad (9)$$

where C_0 is the initial adsorbate concentration (mg/l), m the mass of sorbent per unit volume of particle free adsorbate solution (g/l), K_L the Langmuir constant (obtained by multiplying Q^0 and K_a) (l/mg), β_I the mass transfer coefficient (cm/s) and S is the outer surface of adsorbent per unit volume of particle free slurry (1/cm) [19,21,22]. Eq. (9) was solved by using Polymath 4.1 software and $\beta_I S$ value was determined for the studied adsorption systems.

2.4. Mathews and Weber model

The external mass transfer coefficient can also be calculated by Mathews and Weber (M&W) equation as an alternative method [19] by the equation:

$$C_t/C_0 = \exp \beta_1 St \quad (10)$$

2.5. Thermodynamic parameters

Thermodynamic parameters such as free energy, enthalpy and entropy changes can be estimated using equilibrium constants changing with temperature. The free energy change of the sorption reaction is given by using following equation [23,24]:

$$\Delta G = -RT \ln K_a \quad (11)$$

where R is universal gas constant, K_a the equilibrium constant, T the temperature (K), and ΔG is the free energy change (J/mol). The free energy change indicates the degree of spontaneity of the adsorption process and the higher negative value reflects a more energetically favorable adsorption [25]. The free energy change may be expressed in terms of enthalpy change of adsorption as a function of temperature as follows:

$$\Delta G = \Delta H - T\Delta S \quad (12)$$

Combining Eqs. (11) and (12) and rearranging:

$$\ln K_a = -\Delta H/RT + \Delta S/R \quad (13)$$

where ΔH and ΔS values for dye biosorption can be evaluated from the slope and intercept of the linear plot $\ln K_a$ versus $1/T$ where ΔS and ΔH are change in entropy and enthalpy of adsorption, respectively.

3. Materials and methods

3.1. Biosorbent

E. prolifera, a kind of green seaweed, was obtained from Mediterranian cost in Mersin, Turkey. The seaweed was washed twice with tap water in order to remove adhering insect larvae, soil etc. It was dried in sunlight and then in an oven at 105 °C for 24 h until all the moisture was evaporated, put in distilled water and blended to obtain larger surface area. A stock solution of 10 g/l of biosorbent was prepared.

3.2. Absorbate

The stock solutions of Acid Red 337 and Acid Blue 324 dyes were prepared in 1.0 g/l concentration. Necessary dilutions were made from the stock solution to prepare solutions in the range of concentrations 20–500 mg/l for both dyes. Dyestuffs used were supplied by DyStar with commercial names Telon Blue AFN and Telon Red FRL.

3.3. Batch adsorption studies

The algae solution (10 ml), except for the studies of biosorbent concentration effect, was mixed with 90 ml of the desired dye concentration and initial pH in Erlenmayer flasks. The flasks were agitated on a shaker at constant temperature for 2 h ample time for adsorption equilibrium. Samples (5 ml) of biosorption medium were taken before mixing the biosorbent suspension and dye bearing solution, then at pre-determined time intervals (0.5, 5, 10, 15, 20, 30, 45, 60 and 120 min) for the residual dye concentration in the solution. Samples were centrifuged at 3500 rev/min for 5 min and the supernatant liquid was analysed. Initial pH of each solution was adjusted to the required value with concentrated and diluted H_2SO_4 and NaOH solutions before mixing the biosorbent solution. Experiments were repeated for different initial pH, initial dye concentration, temperature and biosorbent concentration values.

3.4. Analysis

The concentrations of dye remaining in the biosorption medium were determined calorimetrically using a spectrophotometer (Shimadzu UV-160A) at 716 nm for Acid Blue 324 and 529 nm for Acid Red 337.

4. Results and discussion

The biosorption of AR 337 and AB 324 dyes on *E. prolifera* was studied in a batch system and the experimental data were evaluated in many ways such as the determination of the optimum biosorption conditions and thermodynamic parameters, the modelling of the equilibrium and kinetics. The various isotherm, kinetic and diffusion model equations were applied to the experimental data and the constants of these equations were calculated by nonlinear regression analysis rather than linear regression analysis.

4.1. The determination of optimum biosorption conditions

4.1.1. The effect of the initial pH

Initial pH is one of the most important environmental factors influencing not only site dissociation, but also the solution chemistry of the dyes: hydrolysis, complexation by organic and/or inorganic ligands, redox reactions, precipitation are strongly influenced by pH and, on the other side, strongly influence the speciation and the adsorption availability of the dyes. Fig. 1 shows the effect of initial pH on the biosorption of AB 324 and AR 337 onto *E. prolifera* at 30 °C, 100 mg/l of initial dye concentration where optimum initial pH values were determined to be 3.0 for AB 324 and 2.0 for AR 337. The adsorbed AB 324 and AR 337 amounts at optimum initial pH values were found as 55.1 and 59.2 mg/g, respectively. This can be explained on the basis of zero point discharge for biomass. For the algal biomass, the isoelectric point would be at a pH of 3.0 [26,27]. At lower pH below this point, the surface of algae may acquire a positive charge leading to increased anionic dye (direct, acidic, reactive) uptake due to the electrostatic force of attraction. As the pH of the system increases, the number of negatively charged sites increases. A negatively charged surface site on

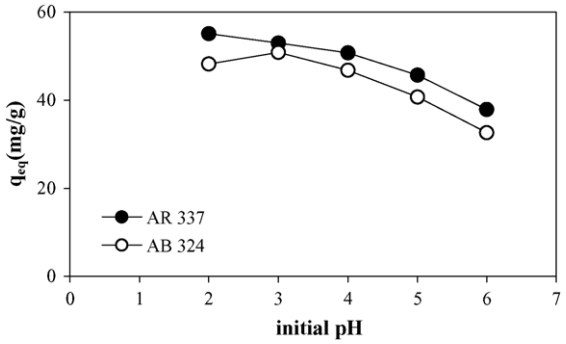

Fig. 1. The effect of initial pH on the equilibrium uptake capacity of *E. prolifera* for AB 324 and AR 337 (X_0 = 1 g/l; temperature, 25 °C; agitation rate, 150 rpm; C_0 = 100 mg/l).

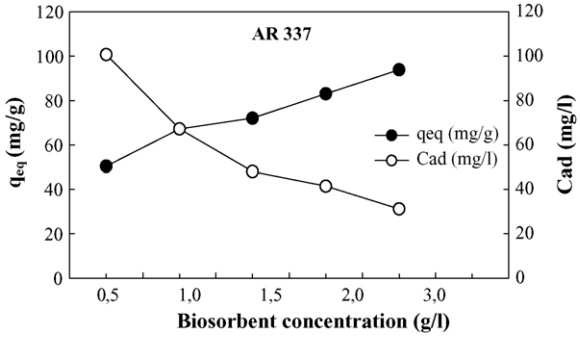

Fig. 3. Effect of biosorbent concentration on the equilibrium uptake capacity and adsorption yield for AR 337 biosorption (temperature, 30 °C; agitation rate,150 rpm; C_o = 100 mg/l; initial pH 2.0).

the biosorbent does not favour the adsorption of dye anions due to the electrostatic repulsion [28].

4.1.2. The effect of the biosorbent concentration

The effect of biosorbent concentration on the dye uptake capacity of *E. prolifera* was investigated for five different biosorbent concentrations in the range of 0.5–3.0 g/l. It is obvious from Fig. 2 that the adsorbed AB 324 concentration increased from 56.0 to 68.9 mg/l while the dye amount adsorbed per unit mass decreased from 112.0 to 23.0 mg/g by increasing the biosorbent concentration from 0.5 to 3.0 g/l. The same trend was also observed for AR 337 as given in Fig. 3. It is readily understood that the number of available adsorption sites increases with an increase in biosorbent concentration and it, therefore results in the increase of adsorbed dye concentration. In fact, in the presence of a high biomass concentration there is a very fast superficial adsorption onto the cells that produces a lower dye concentration in solution than when the cell concentration is lower [26]. The decrease in q_{eq} values may be due to the splitting effect of flux (concentration gradient) between adsorbate and adsorbent with increasing biomass concentration causing a decrease in the amount of dye adsorbed onto unit weight of biomass [28]. Another reason may be due to the particle interaction, such as aggregation, resulted from high biosorbent concentration. Such aggregation would lead to decrease in total surface area of the sorbent and an increase in diffusional path length [21]. As a result, a purification process involving low biosorbent concentration may be suggested for the desired purification since higher uptake values were obtained at low biosorbent concentrations.

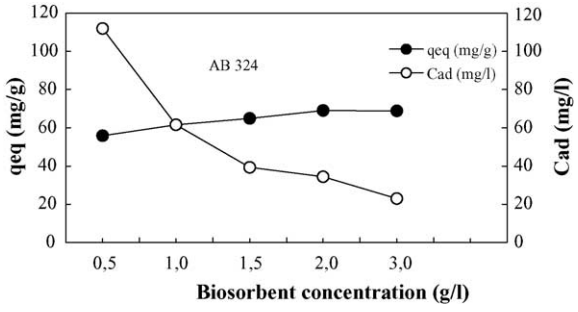

Fig. 2. Effect of biosorbent concentration on the equilibrium uptake capacity and adsorption yield for AB 324 biosorption (temperature, 40 °C; agitation rate, 150 rpm; C_o = 100 mg/l; initial pH 3.0).

4.1.3. The effect of the initial dye concentration

The effect of initial dye concentration on the AB 324 and AR 337 dye biosorption by *E. prolifera* was investigated in the range of 20–500 mg/l of the initial dye concentrations. The variation of the uptake values with initial dye concentrations were depicted in Fig. 4. The uptake amounts increased with increasing initial dye concentrations up to 200 mg/l for AB 324 and AR 337 dyes and then was not changed by further increase in initial dye concentrations suggesting that available sites on the biosorbent are the limiting factor for dye biosorption. At lower dye concentrations, solute concentrations to biosorbent sites ratio is higher, which cause an increase in colour removal [18]. At higher concentrations, lower adsorption yield is due to the saturation of adsorption sites.

4.1.4. The effect of the temperature

The equilibrium uptakes as a function of temperature are given in Fig. 5 for the studied dyes. The equilibrium uptakes increased with increasing temperature up to 25 °C for AB 324 and 30 °C for AR 337 and then decreased. An increase of the equilibrium uptake up to 25 °C for AB 324 and 30 °C for

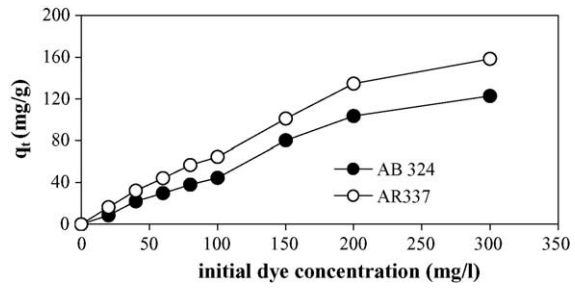

Fig. 4. The effect of initial AB 324 and AR 337 concentration on the adsorption capacity of *E. prolifera* (X_0 = 0.5 g/l, initial pH 3.0, 25 °C, 150 rpm for AB 324 and X_o = 0.5 g/l, initial pH = 2.0, 30 °C, 150 rpm for AR 337).

Table 1
Comparison of the constants obtained from the Langmuir, Freundlich, Redlich–Peterson isotherm models at different temperatures for AB 324

T (°C)	Q^0 (mg/g)	K_a (l/mg)	ERRSQ	K_F	n	ERRSQ	K_{RP} (l/g)	a_{RP} (l/mg)	β	ERRSQ
25	160.59	0.00960	39.73	3.520	1.482	42.57	1.768	0.0904	0.865	37.13
30	131.65	0.00953	47.08	3.077	1.416	43.82	1.527	0.0876	0.709	39.09
40	128.48	0.00945	51.96	2.832	1.118	58.24	1.194	0.0727	0.638	42.73
50	99.26	0.00881	42.84	1.035	1.007	50.72	1.178	0.0699	0.604	35.48

Table 2
Comparison of the constants obtained from the Langmuir, Freundlich, Redlich–Peterson isotherm models at different initial pH values for AB 324

pH	Q^0 (mg/g)	K_a (l/mg)	ERRSQ	K_F	n	ERRSQ	K_{RP} (l/g)	a_{RP} (l/mg)	β	ERRSQ
2	98.79	0.00416	37.48	1.187	0.995	52.45	1.326	0.0722	0.714	40.94
3	160.59	0.00960	39.73	3.520	1.482	42.57	1.768	0.0904	0.865	37.13
4	84.65	0.00514	42.19	0.983	1.002	55.77	0.986	0.63133	0.631	33.50

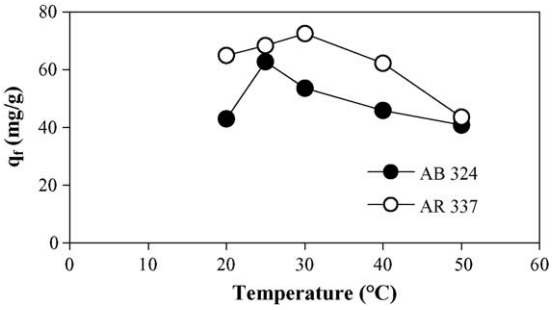

Fig. 5. The effect of temperature on the equilibrium AB 324 and AR 337 sorption capacity of *E. prolifera*.

AR 337 deals with an increase in the biosorption capacity of *E. prolifera* at equilibrium. The decrease of the equilibrium uptakes with further increase in temperature means that the dye biosorption process is exothermic.

4.2. Modelling of the biosorption equilibrium depending on temperature and initial pH

The Langmuir, Freundlich and Redlich–Peterson isotherm models were applied to experimental equilibrium data for AB 324 and AR 337 biosorption at different temperatures and initial pH values. The isotherm constants were determined by using Polymath 4.1 software. The isotherm constants obtained from nonlinear regression analysis at different temperature and initial pH values for AB 324 and AR 337 were given in Tables 1–4, respectively. As seen from Tables 1 and 2, the maximum AB 324 uptake capacity of *E. prolifera* was obtained at 25 °C and initial pH 3.0 as 160.6 mg/g while the maximum AR 337 uptake capacity of *E. prolifera* was obtained at 30 °C and initial pH 2.0 as 210.9 mg/g as can be seen from Tables 3 and 4. It was observed that the uptake capacity of *E. prolifera* for AR 337 was higher than AB 324, resulting in structural differences of this two dyes. For the biosorption of the studied dyes, the K_a values decreased with increasing temperature from optimum temperature to 50 °C, implying that the biosorption equilibrium shifts to the left. The experimental q_{eq} values were found to be smaller than Q^0 indicating that the biosorption of AB 324 and AR 337 on *E. prolifera* is occured by a monolayer type adsorption in which the surface of microorganism is not fully covered.

Regarding that ERRSQ is a criterion of how experimental data fits theoretical isotherms, one can say that Redlich–Peterson isotherm defines best the biosorption of AB 324 and AR 337 on *E. prolifera* with respect to other isotherm models, where the lowest values of ERRSQ were obtained for both dye-biomass systems studied.

It is also observed from Tables 1 and 3 that, the values of n calculated from Freundlich isotherm at different temperatures were found to be very close to each other, indicating that the adsorption intensity was not affected seriously by chang-

Table 3
Comparison of the constants obtained from the Langmuir, Freundlich, Redlich–Peterson isotherm models for AR 337 at different temperatures

T (°C)	Q^0 (mg/g)	K_a (l/mg)	ERRSQ	K_F	n	ERRSQ	K_{RP} (l/g)	a_{RP} (l/mg)	β	ERRSQ
30	210.87	0.0187	100.7	12.663	1.969	79.14	2.117	0.094	0.830	78.94
40	187.72	0.0156	110.88	9.374	1.827	82.49	1.964	0.087	0.736	60.85
50	154.38	0.0099	124.56	7.846	1.658	84.07	1.863	0.065	0.686	65.97

Table 4
Comparison of the constants obtained from the Langmuir, Freundlich, Redlich–Peterson isotherm models for AR 337 at different initial pH values

pH	Q^0 (mg/g)	K_a (l/mg)	ERRSQ	K_F	n	ERRSQ	K_{RP} (l/g)	a_{RP} (l/mg)	β	ERRSQ
2	210.87	0.0187	100.7	12.663	1.969	79.14	2.12	0.094	0.830	78.94
3	167.93	0.0155	96.57	10.841	1.629	88.79	47.86	2.966	0.742	76.47
4	141.94	0.0112	121.86	7.165	1.107	85.63	31.50	1.724	0.681	73.98

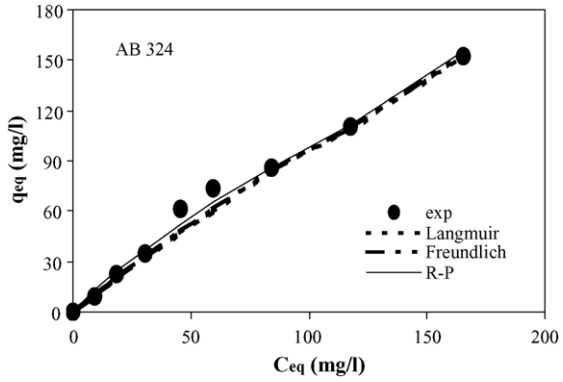

Fig. 6. Comparison of the experimental and modelled isotherms for AB 324 biosorption on *E. prolifera*.

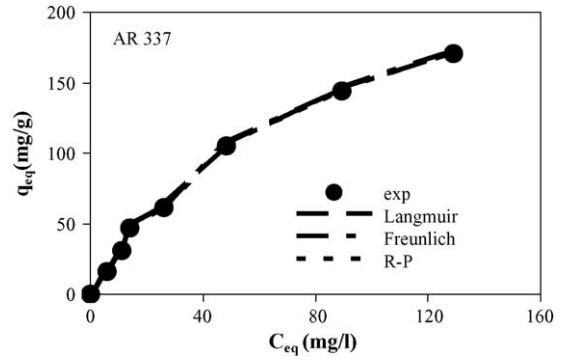

Fig. 7. Comparison of the experimental and modelled isotherms for AR 337 biosorption on *E. prolifera*.

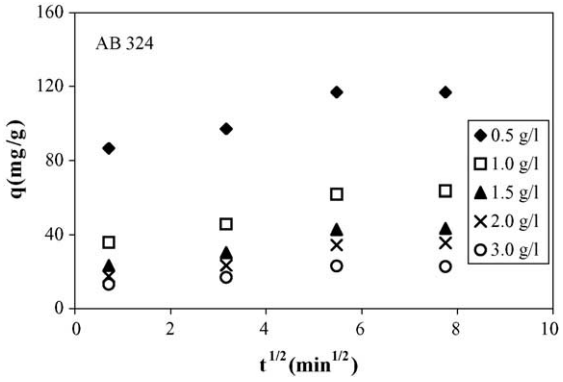

Fig. 8. Plots for the intraparticle diffusion for the biosorption of AB 324 at different biosorbent concentrations.

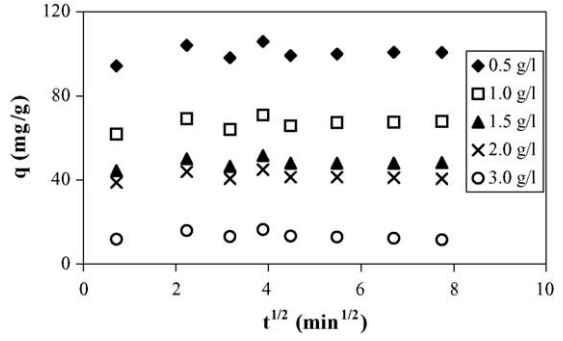

Fig. 9. Plots for the intraparticle diffusion for the biosorption of AR 337 at different biosorbent concentrations.

ing the temperature of adsorption medium. The magnitude of the exponent gives an indication of the favourability of adsorption where *n* values greater than unity represent favorable adsorption condition [14]. The experimental equilibrium data and calculated values from isotherm models were also given in Fig. 6 for AB 324 and Fig. 7 for AR 337, respectively. Furthermore, the temperature and initial pH optima obtained from the isotherm models confirmed the experimental optimum temperature and initial pH for the studied dyes.

4.3. Biosorption mechanism

Weber–Morris model was applied to the biosorption of AB 324 and AR 337 dyes on *E. prolifera* as a function of the biosorbent concentration and the variation of q_t versus $t^{1/2}$ was given in Figs. 8 and 9, respectively. The linear portions of the curves do not pass through the origin indicating that the mechanism of AB 324 and AR 337 removal on *E. prolifera* is complex and both the surface adsorption as well as intraparticle diffusion contribute to the actual adsorption process [15]. The intraparticle rate constants for initial dye concentrations were obtained from the slopes of the lin-

Table 5
Rate constants and regression coefficients obtained from Weber–Morris equation for different initial dye concentrations

	AB324					AR337				
C_0 (mg/l)	20	40	60	80	100	20	40	60	80	100
K	2.642	3.327	4.153	5.778	5.891	0.377	0.572	0.730	1.055	1.268
R^2	0.92	0.97	0.91	0.91	0.95	0.91	0.98	0.94	0.98	0.97

Table 6
Rate constants and regression coefficients obtained from Weber–Morris equation for different biosorbent concentrations

	AB 324					AR 337				
X_0 (g/l)	0.5	1.0	1.5	2.0	3.0	0.5	1.0	1.5	2.0	3.0
K	8.69	5.25	3.94	3.53	1.93	4.76	3.52	2.68	1.04	0.87
R^2	0.95	0.93	0.97	0.96	0.98	0.96	0.99	0.93	0.95	0.97

ear portions of the plots of q_t versus $t^{1/2}$ and the results for initial dye and biosorbent concentrations were presented in Tables 5 and 6, respectively. It was observed that intraparticle rate constant values (K) decreased with increasing biosorbent concentration and increased with initial dye concentration. The increasing trend of intraparticle rate constant values with initial dye concentrations was reported before by various investigators [8,13,24]. The observed increase in K values with increasing initial dye concentration can be explained by the growing effect of driving force, the concentration gradient, while the decrease in K values at higher biosorbent concentrations may be due to agglomeration of biosorbent particles which leads to an increase in mass transfer resistance. As can be seen from Tables 5 and 6, K values obtained for AB 324 at different initial dye and biosorbent concentrations were greater than those obtained for AR 337 dye suggesting that intraparticle diffusion is more effective on the biosorption mechanism of AR 337 on *E. prolifera*.

The external mass transfer coefficients for the biosorption of AB 324 and AR 337 on *E. prolifera* were determined by applying to the experimental data both Frusawa and Smith (F&S) and Mathews and Weber (M&W) models. The $\beta_I S$ values for AB 324 and AR 337 biosorption according to F&S model were calculated to be 0.0527 1/s (ERRSQ = 0.141) and 0.0315 1/s (ERRSQ = 0.188), respectively. For AB 324 and AR 337 biosorption at optimum uptake conditions, the values of $\beta_I S$ obtained from M&W model were determined to be 0.0496 1/s (ERRSQ = 0.4065) and 0.0291 1/s (ERRSQ = 0.5031), respectively. For AB 324 and AR 337 biosorption, the $\beta_I S$ values obtained from F&S and M&W models were found close to each other. These values indicate that the velocity of AB 324 and AR 337 transport from the liquid phase to solid phase is rapid enough to suggest the use of this biosorbent for the treatment of wastewaters enriched in these acidic dyes. The same conclusion was withdrawn by Panday et al. [20].

4.4. Application of the pseudo-second order kinetic model

The nonlinear form (i.e. $q_t = tk_{2,\mathrm{ad}}q_\mathrm{e}^2/(1 + k_{2,\mathrm{ad}}tq_\mathrm{e})$) of the pseudo-second order kinetic rate equation was applied to experimental data at different temperatures for biosorption AB 324 and AR 337 dyes on *E. prolifera* by using Polymath 4.1 software and the $q_{\mathrm{eq,\,cal}}$, $k_{2,\,\mathrm{ad}}$ and ERRSQ values were given in Table 7. The variation of experimental and calculated q_t values with time was given in Fig. 10 for AB 324 and Fig. 11 for AR 337. The pseudo-second order rate constant values decreased with increasing temperature indicating that the biosorption of AR 337 and AB 324 on *E. prolifera* was exothermic in nature while the highest value of $k_{2,\,\mathrm{ad}}$ was obtained at optimum biosorption temperature. The adequate fitting of calculated ($q_{\mathrm{eq,\,cal}}$) and experimental ($q_{\mathrm{eq,\,exp}}$) values for the whole studied range of temperature suggest the applicability of pseudo-second order kinetic model to these biosorption systems.

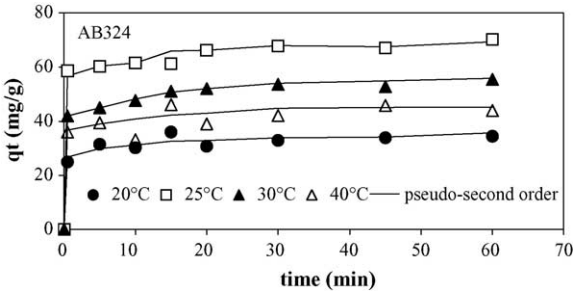

Fig. 10. AB 324 uptake by *E. prolifera* according to the pseudo-second order kinetic model at different temperatures.

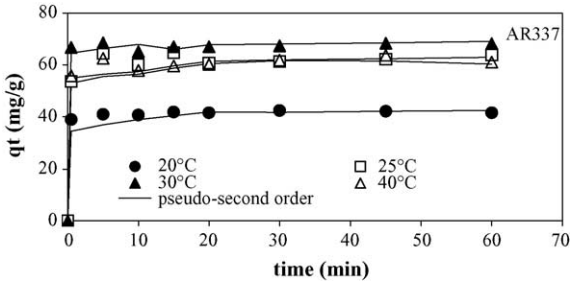

Fig. 11. AR 337 uptake by *E. prolifera* according to the pseudo-second order kinetic model at different temperatures.

4.4.1. The determination of the activation energy

The pseudo-second order rate constant is expressed as a function of temperature by the following Arrhenius type relationship [29]:

$$k_2 = k_0 \exp[-E/RT] \tag{14}$$

Table 7
A comparison of the pseudo-second order rate constants, experimental and calculated q_{eq} values and correlation coefficients obtained at different temperatures for the biosorption of AB 324 and AR 337 by *E. prolifera*

T (°C)	AB 324				AR 337			
	$q_{\mathrm{e,\,exp}}$ (mg/g)	$q_{\mathrm{e,\,cal}}$ (mg/g)	$k_{2,\,\mathrm{ad}}$ (g/mg min)	ERRSQ	$q_{\mathrm{e,\,exp}}$ (mg/g)	$q_{\mathrm{e,\,cal}}$ (mg/g)	$k_{2,\,\mathrm{ad}}$ (g/mg min)	ERRSQ
20	32.93	32.35	0.0292	261.87	41.55	38.77	0.0422	317.32
25	66.27	65.33	0.137	279.12	61.32	61.68	0.0674	245.26
30	53.57	53.67	0.091	197.84	67.29	65.19	0.0931	366.57
40	45.84	45.84	0.0645	91.27	63.73	63.42	0.0871	122.38
50	36.22	36.82	0.0489	117.92	45.05	45.06	0.0598	111.05

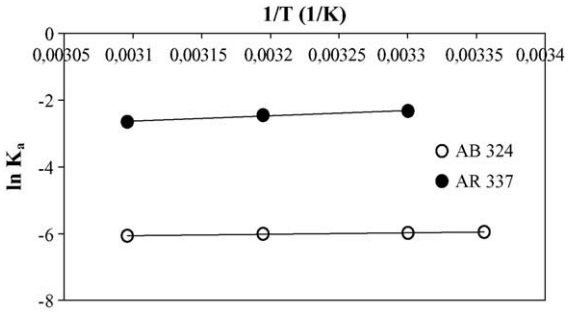

Fig. 12. The variation of $\ln K_a$ with $1/T$ for the biosorption of AR 337 and AB 324.

Table 8
Thermodynamic parameters for the biosorption of AB 324 on *E. prolifera*

Temperature (K)	K_a (l/mg)	ΔG (kJ/mol)	$-T\Delta S$ (kJ/mol)	ΔH (kJ/mol)
298	0.00260	14.53	18.17	−3.64
303	0.00253	14.84	18.48	
313	0.00245	15.45	19.09	
323	0.00231	16.06	19.70	

where k_0 is the temperature independent factor (g/mg min), E the activation energy of sorption (J/mol), R universal gas constant (8.314 J/mol K) and T is the absolute temperature (K). The activation energies for the biosorption of AB 324 and AR 337 were calculated according to Eq. (14) and were found to be −31.46 kJ/mol (ERRSQ = 0.0196) and −19.87 kJ/mol (ERRSQ = 0.0048), respectively. Adsorption is a process in which several parameters can be involved, either related to adsorbent characteristics or to adsorbate structural features as was previously reported by several authors [18,30]. This result arises from the difference in structural features of the two dyes studied. Although AB 324 and AR 337 are both acidic dyes, their molecular weight and shape, molar volume, affinity can affect the uptake capacity of *E. prolifera* as well as parameters related to adsorption process.

4.5. Determination of thermodynamic parameters

For the biosorption of AB 324 and AR 337 dyes on *E. prolifera*, the free energy change (AG) values at different temperatures were calculated from Eq. (11) while the enthalpy (ΔH) and entropy change (ΔS) values were calculated from slope and intercepts of the lines plotted according to Eq. (13) (Fig. 12). ΔG, ΔH and ΔS values for the biosorption of AB 324 and AR 337 on *E. prolifera* were presented in Tables 8 and 9, respectively. Biosorption enthalpies (ΔH) obtained as −3.64 kJ/mol for AB 324 ($R^2 = 0.97$) and −13.58 kJ/mol for AR 337 ($R^2 = 0.97$) indicates that the biosorption of these acidic dyes on *E. prolifera* were exothermic in nature. The biosorption heat (ΔH) for AR 337 was higher than that of AB 324 as its absolute value indicating that the biosorption of AR 337 was more temperature-sensitive. Positive ΔG values indicating a small equilibrium constant were obtained for the biosorption of AB 324 and AR 337 dyes on *E. prolifera*. Whatever the value or sign of ΔG at a defined temperature range, reaction will always occur (though the rate may sometimes be very slow confirming the results of kinetic modelling) until equilibrium is attained [31]. This also explains why we get larger values of q_{eq} for the biosorption of AR 337. Negative values of $T\Delta S$ were obtained for both dyes resulting that the biosorption of AB 324 and AR 337 by *E. prolifera* is reversible.

Table 9
Thermodynamic parameters for the biosorption of AR 337 on *E. prolifera*

Temperature (K)	K_a (l/mg)	ΔG (kJ/mol)	$-T\Delta S$ (kJ/mol)	ΔH (kJ/mol)
303	0.0977	5.81	19.39	−13.58
313	0.0856	6.45	20.03	
323	0.0699	7.09	20.67	

5. Conclusion

The equilibrium and kinetic analysis of the biosorption of two acidic dyes AR 337 and AB 324 on *E. prolifera* has been investigated. *E. prolifera* appeared to be effective for the removal of these acidic dyes from aqueous solutions. The optimum biosorption conditions were determined as the initial pH 3.0 and temperature 25 °C for AB 324; initial pH 2.0 and temperature 30 °C for AR 337, at the initial dye concentration 100 mg/l, biosorbent concentration 0.5 g/l. The Langmuir, Freundlich and Redlich–Peterson adsorption isotherm models were applied to the equilibrium data. The monolayer adsorption capacity of *E. prolifera* was obtained as 160.6 for AB 324 while the maximum AR 337 uptake capacity was 210.9 mg/g at optimum conditions. It was observed that the biosorption data fitted well to the Redlich–Peterson model than the other isotherm models according to ERRSQ analysis. Being not as effective as a commercial activated carbon, *E. prolifera*, a green seaweed has the advantage of being readily abundant and requires little preparation or modification for use as an adsorbent.

Weber–Morris model equation was applied to the experimental data for initial dye and biosorbent concentrations for the two dyes. It was observed that K values decreased with increasing biosorbent concentrations and increased with initial dye concentrations. The external mass transfer coefficient for the biosorption of AB 324 and AR 337 by *E. prolifera* at relating optimum conditions were determined using F&S diffusion model to be 0.0527 and 0.0315 1/s, respectively. The pseudo-second order kinetic model describes the biosorption process with a good fitting. The activation energy values for the biosorption of AB 324 and AR 337 were found to be −31.46 and −19.87 kJ/mol, respectively. Determination of thermodynamic parameters such as enthalpy, entropy and Gibb's free energy changes showed the reversible and exothermic nature of the biosorption of AB 324 and AR 337 by *E. prolifera*.

Acknowledgement

The authors are grateful to TUBİTAK, the Scientific and Technical Research Council of TURKEY, for their financial support of this study (Project No. İÇTAG-Ç090).

References

[1] S.V. Mohan, N.C. Rao, K.K. Prasad, J. Karthikeyan, Treatment of simulated Reactive Yellow 22 (azo) dye effluents using *spyrogyra* species, Waste Manage. 22 (2002) 575–582.
[2] I. Safarik, L. Ptackova, M. Safarikova, Adsorption of dyes on magnetically labeled baker's yeast cells, Eur. Cells Mater. 3 (2) (2002) 52–55.
[3] Y.C. Wong, Y.S. Szeto, W.H. Cheung, G. McKay, Adsorption of acid dyes on chitosan-equilibrium isotherm analyses, Process Biochem. 39 (2004) 693–702.
[4] Y.S. Ho, T.H. Chiang, Y.M. Hsueh, Removal of basic dye from aqueous solution using tree fern as a biosorbent, Process Biochem. 40 (2005) 119–124.
[5] M.M. Nassar, Y.H. Magdy, Removal of different basic dyes from aqueous solutions by adsorption on palm-fruit bunch particles, Chem. Eng. J. 66 (1997) 223–226.
[6] P. Nigam, G. Armour, I.M. Banat, D. Singht, R. Marchant, Physical removal of textile dyes from effluents and solid state fermentation of dye-adsorbed agricultural residues, Bioresource Technol. 72 (2000) 219–226.
[7] S.J. Allen, Q. Gan, R. Matthews, P.A. Jhonson, Comparison of optimized isotherm models for basic dye adsorption by kudzu, Bioresource Technol. 88 (2003) 143–152.
[8] M. Otero, F. Rozada, L.F. Calvo, A.I. Garcia, A. Moran, Kinetic and equilibrium modelling of the methylene blue removal from solution by adsorbent materials produced from sewage sludges, Biochem. Eng. J. 15 (2003) 59–68.
[9] Z. Aksu, S. Tezer, Equilibrium and kinetic modelling of biosorption of Remazol Black B by *Rhizopus arrhizus* in a batch system: effect of temperature, Process Biochem. 36 (2000) 431–439.
[10] A. Özer, D. Özer, Comparative study of the biosorption of Pb(II), Ni(II) and Cr(IV) ions onto *S. Cerevisiae:* determination of biosorption heats, J. Hazard. Mater. B100 (2003) 219–229.
[11] R.S. Juang, F.C. Wu, R.L. Tseng, The ability of activated clay for the adsorption of dyes from aqueous solutions, Environ. Technol. 18 (1997) 525–531.
[12] M.A. Hashim, K.H. Chu, Biosorption of cadmium by brown, green and red seaweeds, Chem. Eng. J. 97 (2004) 249–255.
[13] G. Akkaya, A. Özer, Biosorption of Acid Red 274 (AR 274) on *Dicranella varia*: determination of equilibrium and kinetic model parameters, Process Biochem., in press.
[14] M.S. Chiou, H.Y. Li, Equilibrium and kinetic modelling of adsorption of reactive dye on cross-linked chitosan beads, J. Hazard. Mater. B93 (2002) 233–248.
[15] M. Başıbüyük, C.F. Forster, An examination of the adsorption characteristics of a basic dye (Maxilon Red BL-N) onto live activated sludge system, Pocess Biochem. 38 (2003) 1311–1316.
[16] S. Rengaraj, Y. Kim, C.K. Joo, J. Yi, Removal of copper from aqueous solutions by aminated and protonated mesoporous aluminas: kinetics and equilibrium, J. Colloid Interf. Sci. 273 (2004) 14–21.
[17] P. Waranusantigul, P. Pokethitiyook, M. Kruatrachue, E.S. Upatham, Kinetics of basic dye (methylene blue) biosorption by giant duckweed (*Spirrodella polyrrhiza*), Environ. Pollut. 125 (2003) 385–392.
[18] Z. Aksu, E. Kabasakal, Batch adsorption of 2,4-dichlorophenoxyacetic acid (2,4-D) from aqueous solution by granular activated carbon, Sep. Purif. Technol. 57 (2003) 1–9.
[19] K.K.H. Choy, G. McKay, J.F. Porter, Sorption of acid dyes from effluents using activated carbon resources, Conserv. Recycl. 27 (1999) 57–71.
[20] K.K. Panday, G. Prasad, V.N. Singh, Use of wollastonite for the treatment of Cu(II) rich effluents, Water Air Soil pollut. 27 (1986) 287–296.
[21] A. Shukla, Y. Zhang, P. Dubey, J.L. Margrave, S.S. Shukla, The role of sawdust in the removal of unwanted materials from water, J. Hazad. Mater. B95 (2002) 137–152.
[22] P. Vasudevan, V. Padmanathy, S.C. Dhingra, Kinetics of biosorption of cadmium on Baker's yeast, Bioresource Technol. 89 (2005) 281–287.
[23] T.S. Singh, K.K. Pant, Equilibrium, kinetics and thermodynamic studies for adsorption of As(III) on activated alumina, Sep. Purif. Technol. 36 (2004) 139–147.
[24] C. Namasivayam, D. Kavitha, Removal of Congo Red from water by adsorption onto activated carbon prepared from coir pith an agricultural solid waste, Dyes Pigments 54 (2002) 47–58.
[25] Y.S. Choi, J.H. Cho, Color removal from dye wastewater using vermiculute, Environ. Technol. 17 (1996) 1169–1180.
[26] G. Çetinkaya, Z. Aksu, A. Öztürk, T. Kutsal, A comparative study on heavy metal biosorption characteristics of some algae, Process Biochem. 34 (1999) 885–892.
[27] K.V. Kumar, Ramamurthi, S. Sivanesan, Biosorption of malachite green, a cationic dye onto *Pithophora sp*., a fresh water algae, Dyes Pigments 69 (2006) 74–79.
[28] P.K. Malik, Dye removal from wastewater using activated carbon developed from sawdust: adsorption equilibrium and kinetics, J. Hazad. Mater. B113 (2004) 81–88.
[29] A. Özer, Application of pseudo-second order kinetic model to lead(II) biosorption on *schizomeris leibleinii*, Fresen. Environ. Bull. 12 (2003) 1239–1245.
[30] H. Metivier-Pignon, C. Faur-Brasquet, P. Le Cloirec, Adsorption of dyes onto activated carbon cloths: approach of adsorption mechanisms and coupling of ACC with ultrafiltration to treat coloured wastewaters, Sep. Purif. Technol. 31 (2003) 3–11.
[31] HC. Weber, HP. Meissner, Thermodynamics for Chemical Engineers, Wiley, New York, London, 1963, pp. 367–369.